226 Transactions of the Korean Society of Mechanical Engineers, Vol. 7, No. 2, pp. 226~232, 1983.

<Original>

Quantitative Analysis of Friction Weld Strength by Acoustic Emission

Sae Kyoo Oh*

(Received February 3, 1983)

AE 法에 의한 摩擦熔接强度의 定量解析

吳 世 奎

抄 錄

廻轉數를 熔接變數로 했을 때 異種鋼棒 및 異種鋼管의 摩擦熔接에 있어서 塑性變形中에 發生한 AE (acoustic emission)量과 熔接後의 냉각중에 發生한 AE量의 總量을 測定 解析하고, 熔接表面上에 0.635 mmR의 半圓 노치를 加工했을 때의 熔接部 引張强度를 求하여, AE總量과 熔接部强度와의 相關關係 實驗式 모델을 만들었고, 이들과 關係計算式과의 비교 조사와 95% 신뢰성을 검증하였고, 異種鋼의 摩擦熔接 중에 熔接强度와 品質을 檢出管理할 수 있는 基本資料가 되게 하였다.

1. Introduction

In applying friction welding process, one of the important concerns is the reliable quality monitoring method for a good weld strength in process of production. However, no reliable nondestructive test method is available at present to monitor the weld strength quantitatively in process [1),2)] except the author, et al.'s reports [3),4),5)], even though studies on ultrasonic detection of weld strength were reported[6),7)] but no quantitative relationship was drawn because of considerable scattering of the data.

In this continued study since the former reports[3),4),5)], the relationship between the weld strength and the measurable acoustic emission total counts was analyzed quantitatively. This was possible through relating the direct measurement and analysis of AE counts to the strength (tensile strength) of friction welds of medium carbon low alloy steel bars to sulfurized free machining steel bars and stainless steel tubes to low carbon steel tubes.

2. Specimens and Procedures

The dimensions of welding workpieces and tension test specimens are the same as those in Fig. 1. And the chemical compositions and tensile strength of base metals are listed in

* Member, Department of Mechanical Engineering, National Fisheries University of Busan, Busan, Korea.

Table 1. The friction welding conditions (inertia type) used in this study are revealed in Table 2 including the diameters of workpieces.

The AE transducer location diagram and the block diagram of electronic components for the AE monitoring equipment including the welding parameter-history measuring apparatus are given in Fig. 2-(a) and (b)[3], respectively. A 22.225 mmϕ acoustic emission piezoelectric transducer (Dunegan / Endevco, Model D9203, sensitivity −65 db) was tightly mounted with tape on the jaw, using high vacuum grease on the contacting surface; At such a location as shown in Fig. 2-(a), there was no thermal effect from the interface. The AE equipment was a standard commercial unit (Dunegan/Endevco Model 3000). As shown in Fig. 2-(b), the band pass filter was set to 100 through 300 kHz to remove the background noise, and AE signals were further amplified 35 db with a variable broadband amplifier (0−60 db) after the preamplifier of 40 db[3]. Thereby, the total system gain setting was

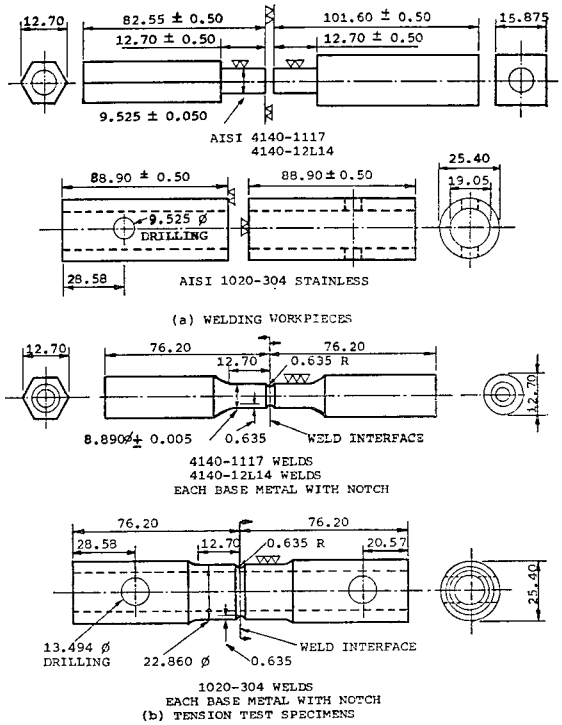

Fig. 1 Welding workpieces and tension test specimens.

Table 1 Chemical compositions and tensile strength of base metals.

Materials (AISI)	Chemical compositions (wt %)									T.S*
	C	Mn	P	S	Pb	Cr	Mo	Ni	Si	σ_T
4140	0.38	0.75	0.04	—	—	0.80	0.15	—	0.20	113.4
1117	0.17	1.00	0.04	0.08	—	—	—	—	—	72.1
12L14	0.15	0.85	0.04	0.26	0.15	—	—	—	—	66.9
1020	0.20	0.45	0.04	0.05	—	—	—	—	—	62.2
304S.S	0.08	2.00	0.04	0.03	—	18.0	—	8.00	0.75	75.5

* Unit : kgf/mm², each specimen with 0.635mm R notch.

Table 2 Welding conditions.

Materials combination (AISI)	Diameter D, mm	Moment of inertia I, kgf·m²	Initial rotating speed n, rpm	Axial pressure p, kgf/mm²
Bar-to-bar 4140-1117 4140-12L14	9.525	0.236	937-3450	12.7, 19.1, 25.5
Tube-to-tube 1020-304S.S	OD 25.40 ID 19.05	0.472	796-2984	8.2

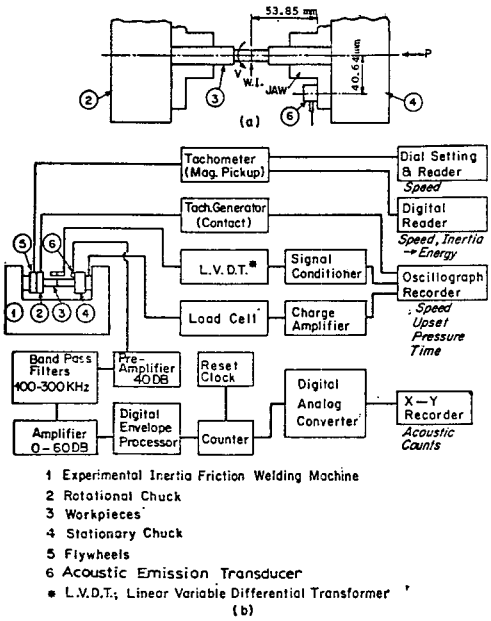

Fig. 2 (a) AE transducer location.
(b) Block diagram of AE monitoring equipment and welding parameters measuring apparatus.

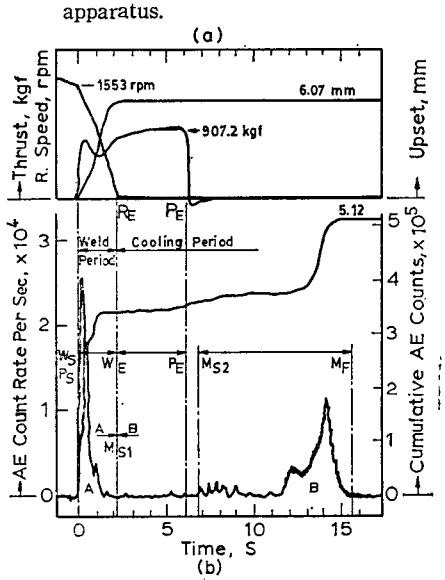

Fig. 3 History of welding parameters and AE measurement in intertia friction welding.

75 db in this study, that is, counting each pulse that exceeded -75 dbv. About eighty workpieces for each metal pair (AISI 4140-1117, 4140-12L14, 1020-304) for welding and measuring AE counts were prepared. Fig. 3[3] shows the typical history of welding parameters and AE measurements in inertia friction welding. The total cumulative AE counts (N, counts) at Zone A of the welding period between welding start (W_S) and welding end (W_E) plus Zone B of the cooling period between martensite formation start (M_S) and finish (M_F) were used for relating to the tensile strength (σ_T, kgf/mm^2) of welded joints, because the AE counts at Zone A result primarily from the plastic deformation during welding and those at Zone B primarily from the martensitic phase transformation during cooling and then the cumulative total AE counts at Zone $A+B$ should be more intimately as a whole correlated to the welded joint properties[4),5)]. The correlated history graphs as those in Fig. 3 were made according to every welding condition and used for analysis of each weldment and AE measurement.

3. Results and Discussions

3.1. Relationship between Weld Strength and Total AE Counts for Zone $A+B$

Fig. 4 shows the relationship between the inertia friction weld strength and total AE counts for Zone $A+B$ of friction welded joints of 9.525 mmϕ bars AISI 4140 to AISI 1117 steels. For comparison the cases of the weld of 25.4 mmϕ (3.175 mm wall) tubes AISI 1020 to AISI 304 stainless steels and 9.525 mmϕ bars AISI 4140 to AISI 12L14 steels are also given in Fig. 4. Regarding to the optimum AE zone (OAZ) for each weld, the OAZ-1 in the case of the weld of AISI 4140 to AISI 1117 is the widest (0.5×10^6 through 2.5×10^6), because of more carbon contents in them and also the martensite-forming-stabilizer Cr content in AISI 4140 resulting in their excellent hardenability. This OAZ-1 is well coincident with the GAZ-1

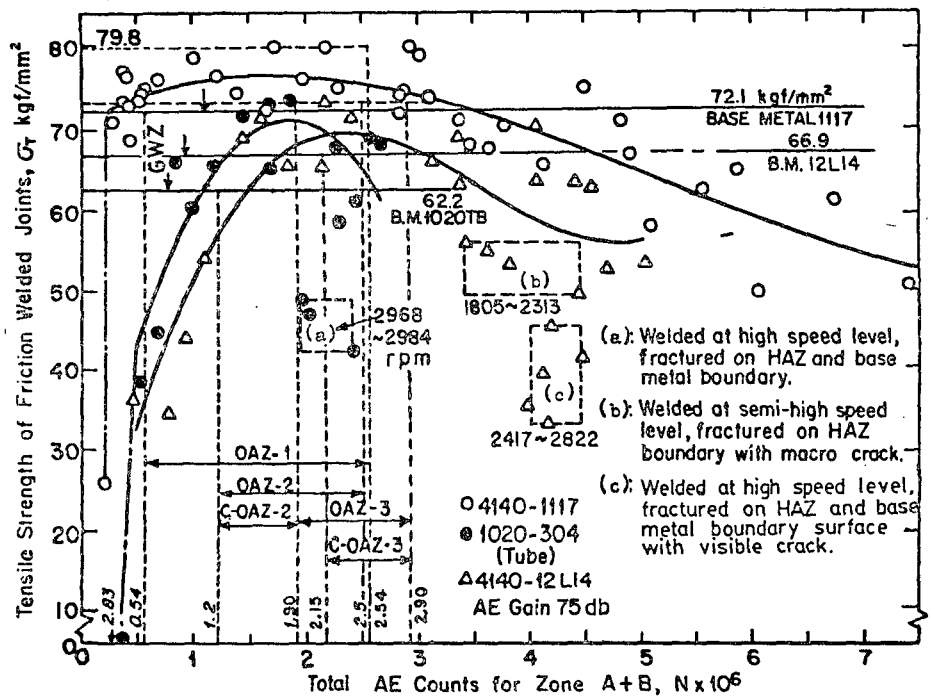

Fig. 4 Relationship between inertia friction weld strength and total AE counts for Zone $A+B$ of friction welded joints of 9.525 mmϕ bars 4140 to 1117 steels, 4140 to 12L14 steels and 25.40 mmϕ (3.175 mm wall) tube 1020 to 304 stainless steels. AE Gain; 75 db.

in the former reports[5),8)]. This means that those have a high reliability.

In the case of welding AISI 1020 to AISI 304 stainless steel tubes, they have especially the area (a) where strength is dropped and total AE counts are very low even though they were welded at high speed level (2968 through 2984 rpm). Those welds were fractured on the boundary area between HAZ and base metal. This must be the dangerous weak points in the view of weld strength. So that, the OAZ-2 (1.2×10^6 through 2.5×10^6 counts) in Fig. 4 should be compensated to the AE range of C-OAZ-2 (1.2×10^6 through 1.9×10^6 counts) for attaining to the GWZ (good welding zone with the joint efficiency more than 100%) for safety quality monitoring and for practical use.

In the case of 4140-to-12L14 welds in Fig. 4, they also have the dropped strength and lowered total AE counts areas (b) and (c) much scattered from the fitted curve exceptionally. The welds in the area (b) welded at semi-high speed level (1805 through 2313 rpm) were fractured on HAZ boundary surface with macro- or micro-crack (as shown in Fig. 5). And also the welds in the area (c) welded at high speed level were fractured on the HAZ and base metal boundary surface with visible crack, and with macro or micro crack (as shown in Fig. 5 (d) and (e) observed by EPMA X-ray images). To avoid these weld defects, the OAZ-3 of AE counts with the range of 1.90×10^6 through 2.90×10^6 counts should be compensated to the C-OAZ-3 with the range of 2.15×10^6 through 2.90×10^6 counts for safety quality monitoring and for practical use, in Fig. 4.

The empirical equations of σ_T-N for 4140-1117, 1020-304 and 4140-12L14 welds are given as the following, computed by the pol-

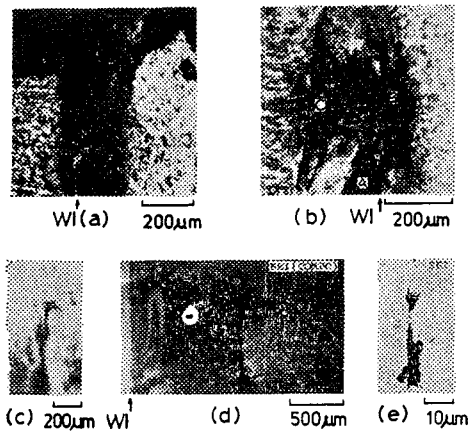

(a) Non-welded periphery of 4140-1117 joint welded at the lowest speet level (937 rpm).
(b) Crack and center defects of 4140-1117 joint welded at the lowest speed level (937 rpm).
(c) Macro crack on HAZ boundary surface of 4140-12L14 joint welded at semi-high speed level (2313 rpm).
(d) Macro crack at boundary area of HAZ and base metal of 4140-12L14 joint welded at high speed level (2617 rpm). (EPMA X-ray image, BEI (COMPO), 20 kV).
(e) Micro crack discontinuities on HAZ boundary of 4140-12L14 joint welded at high speed level (2617 rpm). (EPMA X-ray image, SEI, 20 kV).
Welding conditions; I=0.236 kgf·m², p=12.7 kgf/mm², n=as above.

Fig. 5 Macro and micro photos, and EPMA X-ray images for the discontinuities of the intertia welded joints welded at different speed levels.

ynomial regression analysis, calculating the equation adequacy by the error analysis[5]: For 4140-to-1117 (9.525 mm dia.) welds:

$$\sigma_T = 154.54\times10^{-21}N^3 - 2.3807\times10^{-12}N^2 + 6.6381\times10^{-6}N + 71.39,$$
$$(0.320\times10^6 \leqq N \leqq 7.447\times10^6,\ \text{Eq. adeq.: mean \% error 4.24}) \quad (1)$$

For 1020-304 (25.4 mmϕ, 3.175 mm wall tubes) welds:

$$\sigma_T = -14.779\times10^{-12}N^2 + 54.917\times10^{-6}N + 19.94,$$
$$(0.515\times10^6 \leqq N \leqq 2.649\times10^6,\ \text{Eq. adeq.: mean \% error 8.02}) \quad (2)$$

For 4140 12L14 (9.525 mm dia.) welds:

$$\sigma_T = 1.9987\times10^{-18}N^3 - 21.274\times10^{-12}N^2 + 66.801\times10^{-6}N + 4.12,$$
$$(0.442\times10^6 \leqq N \leqq 5.041\times10^6,\ \text{Eq. adeq.: mean \% error 9.34}) \quad (3)$$

Thus, by the above empirical equations of the $\sigma_T - N$ relationship for the welded joints (AISI 4140-1117, 1020-304 and 4140-12L 14), the general empirical equation form can be modeled as the following cubic ($a \neq 0$) or parabolic ($a=0$) equation depending on materials:

$$\sigma_T = aN^3 + bN^2 + cN + d \quad (4)$$

3.2. Comparison between Empirical and Calculated Equations and 95% Confidence Tests

Fig. 6 shows the comparison between the calculated equations[8] and the empirical equations (1) & (2) : Such calculated equations derived from the combination of empirical $\sigma_T - n$ and $N - n$ are as follows[8],

$$\text{4140-1117}: \sigma_{Tn} = -731.94\times10^{-6}N^{0.75377} + 299.23\times10^{-3}N^{0.37688} + 46.55$$
$$(0.283\times10^6 \leqq N \leqq 7.356\times10^6,\ \text{Mean \% Diff. 0.6\%}) \quad (5)$$

$$\text{1020-304}: \sigma_{Tn} = -13.368\times10^{-6}N^{1.0971} + 73.813\times10^{-3}N^{0.54856} - 30.18$$
$$(0.895\times10^6 \leqq N \leqq 2.484\times10^6,\ \text{Mean \% Diff. 2.02\%}) \quad (6)$$

The maximum mean % difference is only 2.05 %, showing a high reliability.

For their 95% confidence examination, in the case of 4140-1117 welds, the residual sum of squares for the weld strength are computed statistically, and the ANOVA table for testing the lack of fit is calculated as in Table 3. The calculated F-ratios for the lack of fit for both the empirical equations at full range and OAZ-1 of AE and the calculated equation are 1.44, 0.13 and 0.13 which are much smaller than the corresponding values of 3.09, 19.36

Table 3 ANOVA table for testing the lack of fit on the empirical (σ_T-N, mean % error 4.24) and the calculated (σ_{Tn}-N, % difference 0.60) equation models of 4140-1117 welds.

Source	Sum of squares			Degree of freedom			Mean squares			F-ratio		
	Full ra	OAZ-1										
	Empirical		Calculated									
	(1)	(2)	(3)	(1)	(2)	(3)	(1)	(2)	(3)	(1)	(2)	(3)
Residual	545.20	59.59	59.51	37	9	9						
Pure error	87.80	41.24	41.24	8	2	2	10.98	20.62	20.62			
Lack of fit	457.40	18.35	18.27	29	7	7	15.77	2.62	2.61	1.44	0.13	0.13
Remarks	$F_{29,8,0.05}=3.09$ (From F-table, $F_{30,8,0.05}=3.08$ and $F_{24,8,0.05}=3.12$) $F_{7,2,0.05}=19.36$											

and 19.36, respectively from the F-table at 95 percent confidence level. This analysis suggests that not only there is no great danger of lack of fit between all the postulated models and the experimental data in this study, but also it seems possible to monitor the weld strength quantitatively during the process of production by the acoustic emission techniques [3),4),5),8)] more reliably than by the conventional methods[9)].

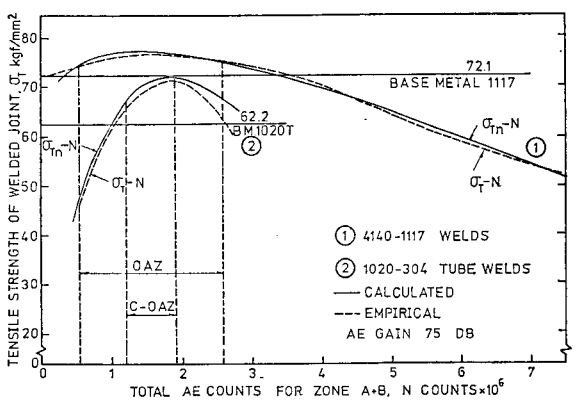

Fig. 6 Comparison between calculated and empirical equations for friction weld strength versus total AE counts of 9.525 mmϕ bar-to-bar (AISI 4140 to 1117) and 25.4 mmϕ (3.175 mm wall) tube-to-bube (AISI 1020 to 304S.S) welds.

4. Conclusions

The results obtained in the study[10)] on Quantitative Analysis of Friction Weld Strength by Acoustic Emission are as follows:

(1) The weld strength can be quantitatively and usefully monitored or controlled in process by using AE techniques because it was confirmed experimentally and quantitatively that the friction weld strength and the total acoustic emission counts have the correlation between them, and the relationship model is expressed as

$\sigma_T=aN^3+bN^2+cN+d$, (depending on materials, $a=0$),

whose maximum mean % difference from the calculated model (σ_{Tn}) is 2.05%, and which has a high reliability, and can be used for in-process monitoring of friction weld strength as a nondestructive monitoring method using AE techniques.

(2) It was confirmed again statistically by error analysis and lack-of-fit testing that the empirical equations for the relationship between the weld strength and the total AE counts computed by the regression analysis using the least squares method have also a reliability at 95% confidence level.

Acknowledgements

The author would like to sincerely thank Professor, Dr. Kuo-King Wang of Cornell University for his useful advice and encourage-

ment, and also a particular acknowledgement should be extended to Professor, Dr. Takeshi Kunio and Professor, Dr. Atsushi Hasui of Keio University for their kind technical advice and discussion during the author's staying at those Universities.

References

1) AWS; Welding Handbook, Vol. 3, pp. 240, AWS, Miami, 1980.
2) JFWRC; Friction Welding, pp. 57, 139, Edited by A. Hasui, Corona, Japan, 1979.
3) S.K.Oh; Friction Weld Strength Analysis by Acoustic Emission Techniques (1), J. of KSME, Vol. 22-3, pp. 184—190, 202, 1982.
4) K.K. Wang, G.R. Reif, S.K. Oh; In-Process Quality Detection of Friction Welds Using Acoustic Emission Techniques, Proc. 63rd Annual AWS Convention, Session 5-A (Apr. 27, 1982). Welding Journal of AWS, Vol. 61-9, September, Welding Research Supplement 312-316-s, 1982.
5) S.K. Oh, A. Hasui, T. Kunio, K.K. Wang; Effects of Inital Energy on Acoustic Emission Relating to Weld Strength in Friction Welding, Transaction of JWS, Vol. 13-2, pp. 15—26, October, 1982. Proc. of 4 th Int. Sym. of JWS, 4 JWS-V-8, Nov. 24-26, pp. 713—718, 1982.
6) K.K. Wang, S. Ahmed; Ultrasonic Detection of Weld Strength for Dissimilar Metal Friction Welds, Proc. of 4th North American Metalworking Research Conf., pp. 384, 1976.
7) S. Ahmed; Ultrasonic Detection of Weld Strength, A Technical Report, Cornell University, USA, 1975.
8) S.K. Oh, K.K. Wang; Effects of Welding Parameters on Weld Strength and Acoustic Emission in Friction Welding, Proc. of the Korean Society of Marine Engineers (Apr. 1982). J. of KOSME, Vol. 7-1, pp. 21—31, 1983.
9) S.K. Oh; Study on Friction Welding of Valve Materials-On Improving the Friction Weld Quality for Exhaustive Valve Materials SUH3-SUH31-, J. of KSME, Vol. 14-3, pp. 221—232, 1974.
10) S.K. Oh; Paper Extracted from Chap. 3 (p. 205—235) in Part Ⅱ of 'Studies on Strength Analysis of Friction Welded Joints and In-Process Monitoring of the Welding Using Acoustic Emission Techniques,' Ph. D. Thesis, Keio University, Japan, 1982.